processes

MDPI

Article

Quantitative Evaluation Method for Sedimentation Stability of Oil Well Workover Fluids by Spectral Analysis

Wenzhe Li [1], Yufei Li [1], Kui Zhang [2], Hao Gong [1], Naiyan Zhang [1], Rui Su [3] and Junlin Su [3,*]

[1] China National Petroleum Corporation Southwest Oil and Gas Field Engineering Institute, Chengdu 610017, China
[2] China National Petroleum Corporation Beijing Engineering Institute, Chengdu 611930, China
[3] State Key Laboratory for Oil/Gas Reservoir Geology and Exploitation Development, Southwest Petroleum University, Chengdu 610500, China
* Correspondence: sjlzr2006@126.com

Abstract

Under long-term high-temperature and static conditions, high-density workover fluid settles, increasing the risks of workover operations. In order to achieve a quantitative assessment of the sedimentation stability of oil well workover fluids, this study adopted spectral analysis to conduct stability tests on water dispersions of barite with different concentrations. Meanwhile, a comprehensive assessment was conducted on the sedimentation rate of the well repair fluid, the size of solid particles and the changes in the thickness of the sedimentary layer in 1# Well, 2# Well and 3# Well. With the increase in barite concentration, its sedimentation behavior changes from free sedimentation at low concentrations to flocculation sedimentation at high concentrations, and the sedimentation rate shows a slowing trend. The increase in sedimentation rate is positively correlated with the increase in density, and the intensity of the initial backscattered light at the bottom of the well also increases accordingly. In addition, during the sedimentation process of sediment, the variation pattern of particle velocity shows the characteristics of being relatively fast in the early stage and gradually accelerating in the middle and later stages. The results show that the average particle size of barite solution is 4.93 μm, and the average particle size of the three workover fluids is 87.5 μm. The deposition thickness range of barite solution is 5–50 mm, and that of the three workover fluids is 25–51.58 mm. It provides data support for the rapid quantitative evaluation of the long-term stability of oil well workover fluids.

Keywords: barite; sedimentation stability; spectral analysis; workover fluids

check for updates

Academic Editor: Václav Uruba

Received: 23 September 2025
Revised: 21 October 2025
Accepted: 22 October 2025
Published: 29 October 2025

Citation: Li, W.; Li, Y.; Zhang, K.; Gong, H.; Zhang, N.; Su, R.; Su, J. Quantitative Evaluation Method for Sedimentation Stability of Oil Well Workover Fluids by Spectral Analysis. *Processes* **2025**, *13*, 3469. https://doi.org/10.3390/pr13113469

Copyright: © 2025 by the authors. Licensee MDPI, Basel, Switzerland. This article is an open access article distributed under the terms and conditions of the Creative Commons Attribution (CC BY) license (https://creativecommons.org/licenses/by/4.0/).

1. Introduction

With the continuous increase in oil and gas exploration, the number of deep wells, ultra-deep wells and high-temperature exploration wells is constantly rising, and the requirements for the temperature resistance and thermal stability of oil-based workover fluids is also becoming higher and higher. Under long-term high-temperature and static conditions, high-density workover fluids may undergo static settlement, increasing the risks of workover operations [1–4]. Therefore, it is of great significance to study the sedimentation stability of solid weighting materials in workover fluids.

Commonly, the factors influencing the sagging of solid weighting materials in workover fluids are as follows: the properties of the weighting materials, including particle size and density, fluid rheology, as well as environmental conditions such as temperature,

pressure and time, all affect the sag of the weighting materials [5,6]. Due to its many advantages such as high specific gravity (4.2~4.4), low production cost and small environmental impact, barite is commonly used as a weighting agent [7,8]. However, when using barite, solid particle sedimentation is a common problem, and this phenomenon is called barite sagging [9,10]. In this field, scholars have conducted extensive research on experimental methods and theoretical models for evaluating the sagging of weighting materials.

Jamrozik et al. [11] used an optical Turbiscan Lab analyzer to measure the sedimentation stability of the samples. By quantifying the changes in light intensity measured at various heights of the scanned samples before and after the test, they can visually compare the stability differences between the samples, thereby determining the Turbiscan Stability Index (TSI). The smaller the TSI value, the better the stability of the system. The sedimentation stability test of drilling fluid at 20 °C to 60 °C for 24 h shows that the sedimentation stability of the drilling fluid decreases with the increase in temperature. Santos et al. [12] used synthetic olefin-based drilling fluids in the experiment and employed gamma-ray attenuation technology to monitor the distribution of solid concentrations. Ofei et al. [13] reported a method for quantitatively evaluating the static sag stability of oil-based drilling fluids using gamma-ray attenuation. This method uses cesium-137 isotope as the gamma source and is equipped with a NaI detector with a diameter of 5 cm for measuring transmitted gamma radiation, then records the variation in the count over time and uses it to calculate the density of the fluid. Zeng and Bouguetta [14] proposed an evaluation index for static ptosis stability, known as the Static stratification Index (SSI). This method involves stratifying the cooled completion fluid in the aging tank, measuring the density and volume of different sections and ultimately calculating the SSI. In addition, researchers have also developed a variety of mathematical models. For instance, Bern et al. [10] developed a simplified model based on empirical analysis using continuum mechanics to describe the sagging trend of barite in different fluid types. Ribeiro et al. [15] also proposed a two-phase model based on the mass and momentum conservation equations, which describes the sagging of barite in drilling fluid. At present, for the static settlement stability of workover fluids, the sagging factor method is mostly adopted to evaluate the settlement trend of workover fluids [16]. However, the existing quantitative testing methods are unable to rapidly and quantitatively predict the sedimentation stability parameters of workover fluids. In addition, compared with light scattering, the light transmission method is not sensitive to low-concentration or fine-particle samples, cannot distinguish between particle concentration and particle size changes and is easily interfered with by sample color and cannot identify particle agglomeration behavior. Its detection accuracy and information dimension are both worse.

This study aims to simultaneously measure the upper and lower layers of workover fluid using a spectral instrument. By taking advantage of the different transmission and reflection properties of incident light in different fluid systems, the sedimentation stability data of the sample to be tested is obtained. Because the spectral test of the stability of downhole working fluids is an important technical means to evaluate the stability of workover fluids in well testing operations [17], the spectral characteristic changes in workover fluids at different time points were tested and analyzed by the BeScan Lab instrument, and a comprehensive assessment was conducted on the sedimentation rate, solid particle size and sedimentary layer thickness changes in three oil well operation fluids. The results show that with the increase in barite concentration, its sedimentation behavior changes from free sedimentation at low concentrations to flocculation sedimentation at high concentrations, and the sedimentation rate shows a slowing trend. The increase in sedimentation rate is positively correlated with the increase in density, and the intensity of the initial backscattered light at the bottom of the well also increases accordingly. In

addition, the velocity variation pattern of particles during the sedimentation process shows the characteristics of being relatively fast in the early stage and gradually accelerating in the middle and later stages. This discovery provides a direction for the rapid quantitative assessment of the long-term stability of workover fluids. This method can effectively monitor and adjust the performance of the workover fluid, providing a solid foundation for ensuring the smooth progress of the workover operation.

2. Materials and Methods

2.1. Materials

The sedimentation stability of the solution was tested using the BeScan Lab stability analyzer (Dandong Bettersize Instruments Ltd., Beijing, China). The detection angle is 0° transmission and 135° backscattering, the light source is 850 nm and the detection mode is highly scanned. The equipment size (length × height × width) is 46 cm × 26 cm × 28 cm.

2.2. Principle of Instrument Testing

When an object moves at a constant speed in a viscous fluid, a layer of adhering liquid forms on the surface of the object. There is internal friction between this liquid layer and the adjacent liquid layer, so the object must overcome this resistance during movement. If the object is spherical, the liquid moves in laminar flow relative to the sphere (Figure 1).

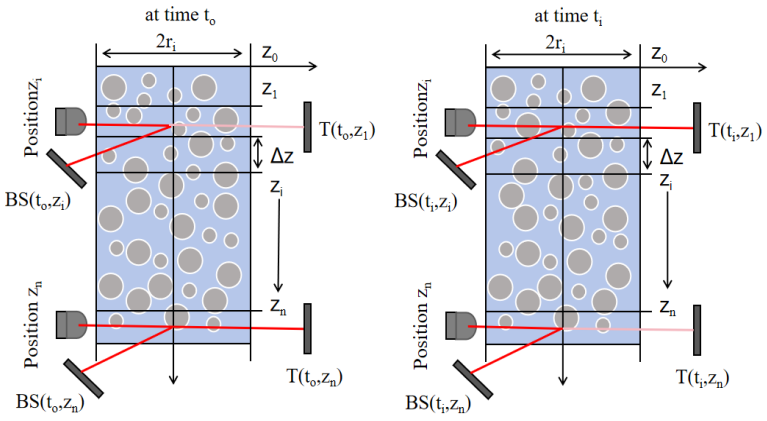

Figure 1. Schematic diagram of particle migration under gravity.

Under the condition that the system reaches equilibrium (i.e., particles reach terminal velocity) and all particles have the same hydrodynamic parameters (i.e., there is only one dispersed material), the migration velocity vs. (D, z, t) can be described using Stokes' law [18], assuming a dilute medium and spherical particles. Stokes' law is not applicable to concentrated dispersion systems due to the influence of adjacent particles. By introducing the hindrance factor h (ϕ) [19], Stokes' law can be modified as follows. According to the Mie theory and Stokes formula, the sedimentation rate of particles can be represented as follows:

$$V(\varnothing, d) = \frac{|\rho_p - \rho_c| \times g \times d^2}{18 \times v \times \rho_c} \cdot \frac{(1-\varnothing)}{\left[1 + \frac{4.6\varnothing}{(1-\varnothing)^3}\right]} \quad (1)$$

In this study, the particle migration rate (V) is measured in meters per second (m/s), the density of the continuous phase (ρ_c) in kilograms per cubic meter (kg/m^3), the particle density (ρ_p) also in kilograms per cubic meter (kg/m^3), the gravitational acceleration (g) is 9.81 m/s^2, the average particle diameter (d) is measured in micrometers (μm), the viscosity of the continuous phase (ν) in centipoise (cP) and the volume fraction (ϕ) is a dimensionless parameter.

The proposed hindrance factor expression is based on the assumption of monodisperse spheres, and therefore deviations may occur in highly concentrated and highly polydisperse liquid dispersion systems. The development of complex numerical models [20] has been reinvigorated for the precise simulation of concentrated dispersions of polydisperse hard spheres settling or condensing. Nonetheless, the proposed expressions generally provide satisfactory results [21]. When the average path length L (f, d) of photons exceeds the wavelength L of the incident radiation, the propagation of light in a randomly dispersed medium is considered independent or incoherent [22]: (for isotropic Rayleigh scattering g = 0, for Mie scattering with sizes larger than the wavelength $0 \leq g \leq 1$) [23].

For anisotropic scattering, we further define the photon transport length $L^* = L/(1 - g)$, which represents a decorrelation length, beyond which photons will forget the direction of the incident beam and the scattering pattern of individual particles [24–30].

When an electromagnetic wave is emitted into a transparent sample placed in a glass test chamber, the resulting emission spot consists of two parts (Figure 2).

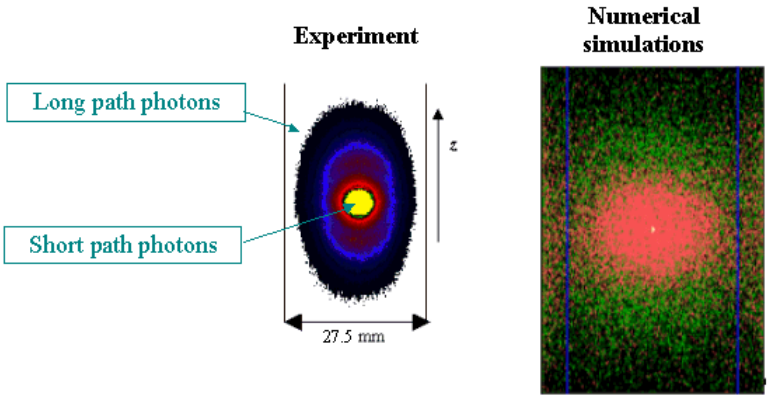

Figure 2. Central part of the short-step photons and the circular part of the long-step photons.

The instrument (BeScan Lab Stability Analyzer) mainly analyzes the central part of the reflected light spot; therefore, the measured reflected light flux BS is related to λ* (BS is approximately inversely proportional to the square root of λ*). Given the known system density, system viscosity, particle density and particle size, the sedimentation velocity of the particles can be calculated.

$$BS \approx \frac{1}{\sqrt{\lambda^*}} = \sqrt{\frac{3\varnothing(1-g)Qs}{2d}} \tag{2}$$

$$\lambda^*(d, \varnothing) = \frac{2d}{3\varnothing(1-g)Qs} \tag{3}$$

In the formula: BS represents the backscattered luminous flux; λ* is the average free path of photons in the dispersion system; φ is the particle volume concentration; d is the average particle size; g(d) and Qs(d) are optical parameters given by Mie theory [31–37]. Given the particle volume concentration φ and the measured backscattered luminous flux BS, the average particle size d can be calculated. With the known particle volume concentration φ, initial system viscosity and sedimentation velocity, the thickness of the particle sedimentation layer H can be calculated.

$$H(\pi D^2) = \frac{1 + 2.5\varnothing + 7.6\varnothing^{0.5}}{(1 - 0.65\varnothing)\mu^{\alpha}} + V(\varnothing, d)t \tag{4}$$

In the formula: H—thickness of the sediment layer (mm); D—pipe radius (mm); φ—volume percentage; v—particle migration rate (m/s); d—average particle size (μm);

μ—average particle size (cP); α-coefficient. Based on the above formula, the corresponding settling rate, settling thickness and settling particle size can be calculated, and then the settling behavior of the oil well work fluid can be quantitatively analyzed [38,39].

2.3. Barite Water Dispersion System Test Steps

Inject the barite water dispersion sample to be tested into the visual sample tube, ensuring that the sample volume does not exceed two-thirds of the tube's capacity (Figure 3). Tighten the cap of the sample tube. At room temperature, samples 1–8 (Table 1) were scanned at 15 min intervals, and the backscattering intensity values of each scan were recorded.



Figure 3. Settling images of barite with different contents.

Table 1. Experimental scheme for testing the average settlement rate of particles in oil testing fluid.

Number	Sample	Density (g/cm^3)	Settlement Temperature (°C)	Sedimentation Time
1	2% Barite Water Dispersion	1.02	25	15 min
2	5% Barite Water Dispersion	1.05	25	15 min
3	8% Barite Water Dispersion	1.08	25	15 min
4	10% Barite Water Dispersion	1.10	25	15 min
5	13% Barite Water Dispersion	1.13	25	15 min
6	15% Barite Water Dispersion	1.15	25	15 min
7	18% Barite Water Dispersion	1.18	25	15 min
8	20% Barite Water Dispersion	1.20	25	15 min
9	1# Well oil testing work fluid	1.87	92.4	15 days
10	2# Well oil testing work fluid	1.47	132	15 days
11	3# Well oil testing work fluid	2.15	105	15 days

By analyzing these data, the sedimentation rate of the sample can be calculated, and its stability can be assessed. During the experiment, it is also important to maintain a constant temperature of the sample to ensure the accuracy of the test results. After completing all scans, organize the data and plot a graph showing the change in backscattering intensity over time, thereby visually demonstrating the sedimentation characteristics of different concentrations of barite water dispersion liquid.

2.4. Oil Well Fluid Settlement Evaluation Experimental Procedure

Place fifteen sets of three different types of oil samples each into a pressure-resistant boiling prevention device and process them under different temperature conditions as

shown in Table 1. Then, place the device in an oven for a settlement experiment lasting 15 days (Figure 4). During the experiment, it is essential to ensure that each oil sample maintains a constant temperature under its respective temperature conditions. Every 48 h, remove one sample from the device and test it using the same method as in Section 2.2.

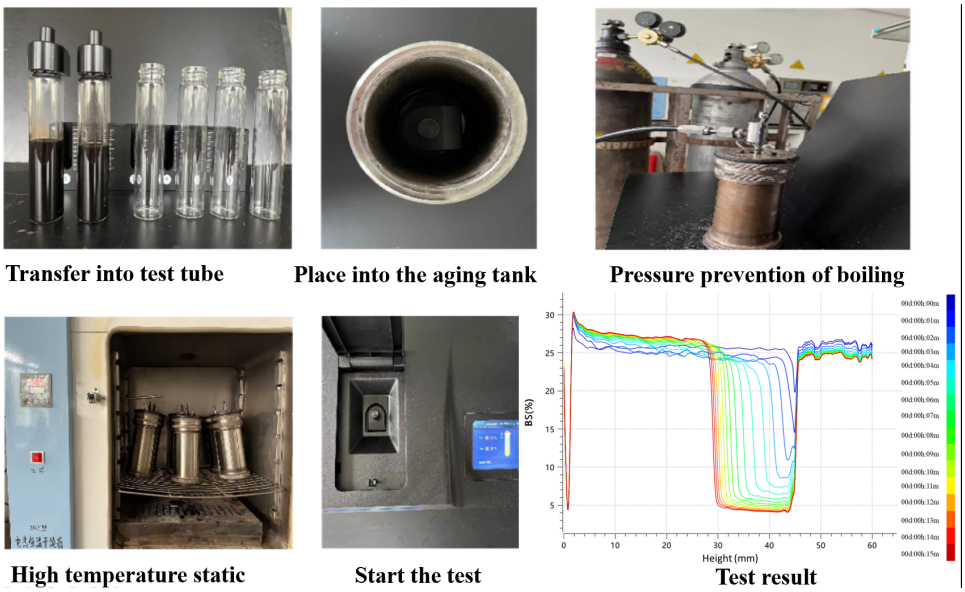

Figure 4. Settlement stability test steps of the oil test working fluid.

3. Results and Discussion

3.1. Backscattering Intensity Variation

Figures 5 and 6 show that the difference in light intensity at 15 days below the bottom, 2 cm from the bottom, indicates that the greater the difference in reflected light intensity at different heights at the same time, the faster the settling velocity, and the greater the density, the greater the initial backscattering light intensity at the bottom. It also shows that the pattern of particle settling velocity from early to middle to late stages is that the earlier the settling velocity is greater, the faster the rate in the middle and later stages. This provides data support for the rapid quantitative assessment of the long-term stability of working fluids.

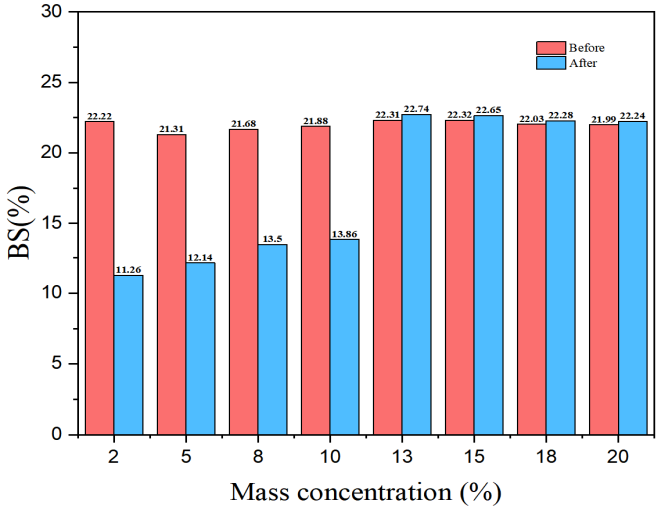

Figure 5. Backscattered light intensity change of 2 cm barite water dispersion at the bottom.

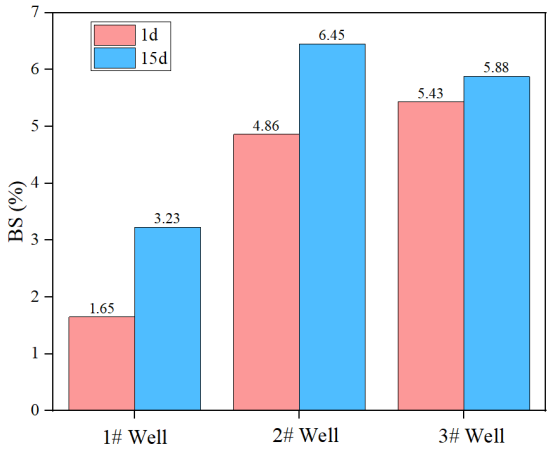

Figure 6. The intensity changes in backscattered light of the three oil test solutions.

3.2. Settlement Rate

Figure 7 shows the variation in settling rates of different oil well workover fluids over a period of 15 days. It can be observed that within the 15-day observation period, the settling rates of barite oil well workover fluids at different concentrations exhibit significant differences. Specifically, the initial sedimentation rate of low-concentration barite solution (such as 2%) is relatively fast, but it gradually slows down and tends to stabilize over time. In contrast, higher concentration barite solutions (such as 20%) display more complex settling behavior, with slower initial settling rates, which then gradually increase and eventually reach a relatively stable value after a certain period. Additionally, the trend of settling rate changes is closely related to the content of barite. As the concentration of barite increases, the fluctuation range of the settling rate also increases accordingly. This may be due to the enhanced interaction between high concentration barite particles, leading to more pronounced aggregation and flocculation phenomena during the settling process.

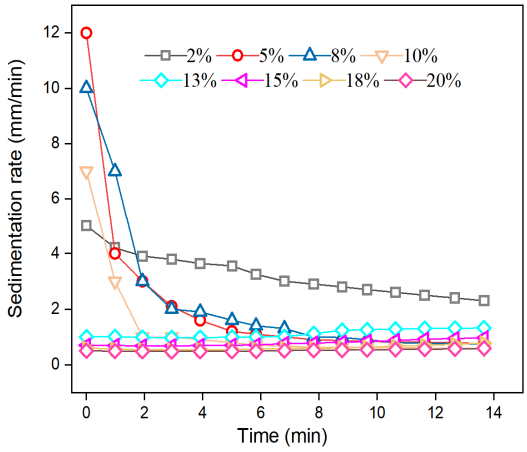

Figure 7. Settlement rate of barite water dispersion.

Figure 8 shows that the sedimentation rate does not decrease linearly by comparing the sedimentation rates at different aging time points. At the beginning of aging, the sedimentation rate decreases rapidly, but as the aging time is further extended, the trend of the sedimentation rate decrease gradually slows down. This is because in the early stages of aging, unstable particles in the working fluid settle quickly, and as time goes on, the remaining particles become more stable, thus slowing down the sedimentation rate. With the increase in aging time, the density of the working fluid also decreases, which may be related to the sedimentation of particles. The sedimentation of particles leads to a reduction

in the solid particle content in the working fluid, thereby affecting the overall density of the working fluid.

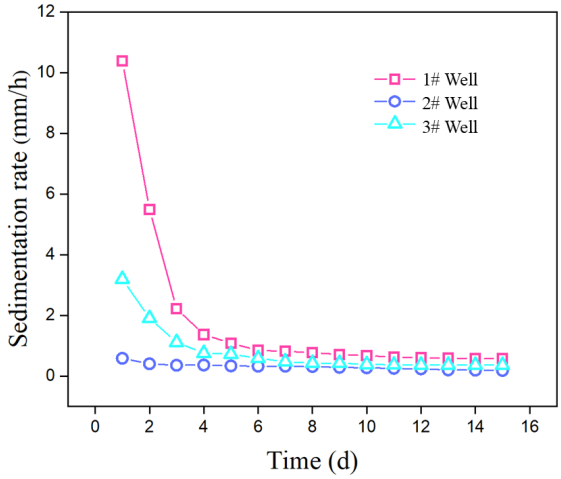

Figure 8. The sedimentation rate of the three different oil test working solutions.

3.3. Particle Size Analysis

Figure 9 shows the change in average particle size of barite water dispersions at different concentrations. From the graph, it can be observed that the average particle size first increases and then decreases with the increase in barite concentration. This may be due to the fact that at low concentrations barite particles are more uniformly dispersed. As the concentration increases, particles begin to aggregate, leading to an increase in particle size. However, when the concentration further increases to a certain extent, the interaction forces between particles reach saturation, aggregation weakens and the particle size begins to decrease. Additionally, the change in particle size corresponds with the trend of sedimentation rate changes. During the phase of faster sedimentation, larger particles lead to higher sedimentation rates.

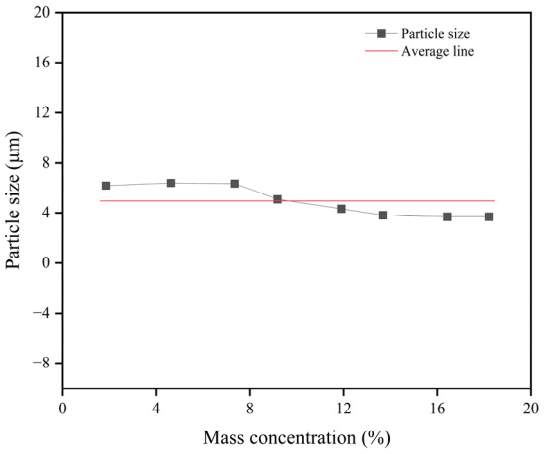

Figure 9. Average particle size of barite water dispersion at different concentrations.

Figure 10 shows that after aging the sample at high temperatures for different periods, the average particle size of the solid phase particles exhibits a certain degree of fluctuation. As the aging time increases, the particle size first increases and then decreases. This fluctuation may be related to the decomposition and recombination of chemical components in the working fluid, indicating that the stability of the working fluid is affected under high-temperature conditions. Changes in particle size may also be related to the aggregation

and dispersion of solid phase particles in the working fluid. In the early stages of aging, particles may disperse due to thermal motion, and over time, as thermal motion weakens, particles may gradually aggregate, leading to an increase in particle size.

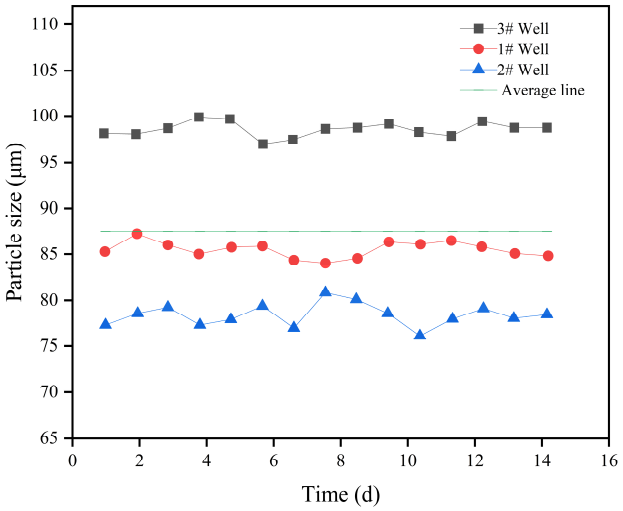

Figure 10. Analysis of particle size for different oil testing fluids.

3.4. Settlement Thickness Analysis

Figure 11 shows a curve graph of the settlement thickness over time. In the initial stage, the settlement thickness increases rapidly because the barite particles settle quickly under the force of gravity. As time goes on, the settlement rate gradually slows down, and the increase in settlement thickness becomes more gradual, indicating that particle deposition is gradually reaching a balanced state. The rapid increase in settlement thickness over a short period of time suggests that the particles in the working fluid tend to agglomerate and have poor stability. Conversely, if the settlement thickness increases slowly and the final equilibrium thickness is small, it indicates that the working fluid has good stability.

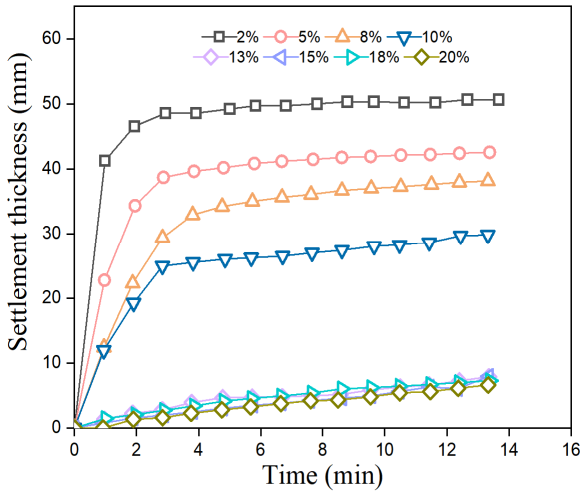

Figure 11. Settlement thickness variation over time.

Figure 12 shows the changes in the settling thickness of different oil testing work fluids over a period of 15 days. With the extension of aging time, the thickness of the sediment layer shows a gradual decreasing trend. Taking 3# Well as an example, the thickness of the sediment layer is 51.58 mm on the first day, which decreases to 44.39 mm by the 15th day. This indicates that under high-temperature conditions, certain components in the

work fluid may have undergone decomposition or polymerization reactions, leading to a reduction in the amount of sediment. The thickness of the sediment layer decreases rapidly in the initial stage, then the rate of decrease gradually slows down, and eventually stabilizes. This change may be related to the thermal stability of different components in the work fluid, where some components may react quickly in the initial stage, while others require a longer time to reach thermal equilibrium.

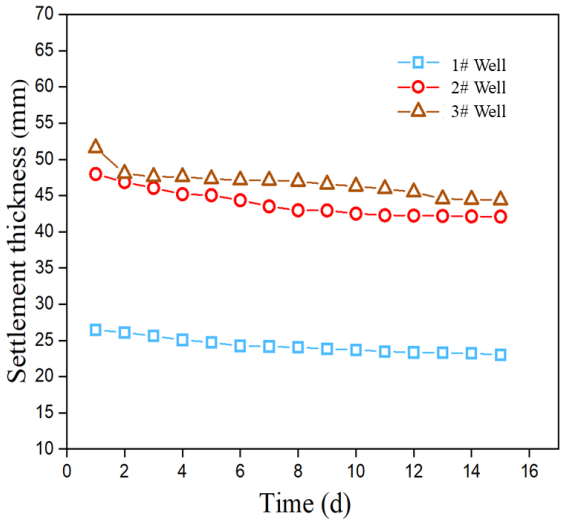

Figure 12. Variation in the settling thickness of different oil testing work fluids within 15 days.

4. Conclusions

This study indicates that the stability of the working fluid under high-temperature conditions is closely related to the time factor. The experimental results show that there is a certain correlation between the stable value of sedimentation rate and the content of barite. Within the low concentration range, the stable value of sedimentation rate is relatively low. However, within the high concentration range, the stable value of sedimentation rate is relatively high. In addition, the content of barite has a significant impact on the stability of the working solution: as the content of barite increases, the stability of the working solution first rises and then falls, indicating that there exists a specific concentration range that optimizes the stability of the working solution. It is worth noting that the stability of the working fluid is also related to the particle size distribution. The smaller the particle size, the slower the sedimentation rate and the better the stability. Therefore, by adjusting the barite content and particle size, the stability of the working fluid can be effectively regulated to meet the adaptability requirements of different working environments.

Author Contributions: W.L.: Data curation, Formal analysis. Y.L.: Investigation, Methodology, Writing—Review and Editing. K.Z.: Investigation, Writing—Review and Editing. H.G.: Writing—Review and Editing. N.Z.: Formal analysis, Writing—Original Draft, Formal analysis. R.S.: Writing—Original Draft, Formal analysis, Investigation. J.S.: Investigation, Methodology, Project administration. All authors have read and agreed to the published version of the manuscript.

Funding: This research was funded by the Science and Technology Cooperation Project of the CNPC-SWPU Innovation Alliance (No. 2020CX040201).

Data Availability Statement: Data will be made available on request.

Conflicts of Interest: Authors Wenzhe Li, Yufei Li, Hao Gong, and Naiyan Zhang were employed by the China National Petroleum Corporation Southwest Oil and Gas Field Engineering Institute. Author Kui Zhang was employed by the China National Petroleum Corporation Beijing Engineering

Institute. The remaining authors declare that the research was conducted in the absence of any commercial or financial relationships that could be construed as a potential conflict of interest.

References

1. Adjei, S.; Elkaktatny, S.; Sokama-Neuyam, Y.A.; Sarkodie, K.; Quaye, J.A. Evaluation and remediation techniques for barite sagging: A review. *Geoenergy Sci. Eng.* **2023**, *225*, 211731. [CrossRef]
2. Alade, O.; Mahmoud, M.; Al-Nakhli, A. Rheological studies and numerical investigation of barite sag potential of drilling fluids with thermochemical fluid additive using computational fluid dynamics (CFD). *J. Pet. Sci. Eng.* **2023**, *220*, 111179. [CrossRef]
3. Rocha, R.R.; Oechsler, B.F.; Meleiro, L.A.C.; Fagundes, F.M.; Calada, L.A. Settling of weighting agents in non-Newtonian fluids to off-shore drilling wells: Modeling, parameter estimation and analysis of constitutive equations. *J. Pet. Sci. Eng.* **2019**, *184*, 106535. [CrossRef]
4. Vrålstad, T.; Saasen, A.; Fjær, E.; Øia, T.; Ytrehus, J.D.; Khalifeh, M. Plug & abandonment of offshore wells: Ensuring long-term well integrity and cost-efficiency. *J. Pet. Sci. Eng.* **2019**, *173*, 478–491. [CrossRef]
5. Gautam, S.; Guria, C.; Rajak, V.K. A state of the art review on the performance of high-pressure and high-temperature drilling fluids: Towards understanding the structure-property relationship of drilling fluid additives. *J. Pet. Sci. Eng.* **2022**, *213*, 110318. [CrossRef]
6. Wang, G.; Wang, J.; Tan, K. Experimental and modelling studies on static sag of solid weighting powders in Polysulfonate workover fluids at high temperature and high pressure. *Petroleum* **2025**, *11*, 13–22. [CrossRef]
7. Geri, B.S.B.; Mahmoud, M.; Abdulraheem, A.; Al-Mutairi, S.H.; Elkatatny, S.M.; Shawabkeh, R.A. Single stage filter cake removal of barite weighted water based drilling fluid. *J. Pet. Sci. Eng.* **2017**, *149*, 476–484. [CrossRef]
8. Pozebon, D.; Lima, E.C.; Maia, S.M.; Fachel, J.M. Heavy metals contribution of non-aqueous fluids used in offshore oil drilling. *Fuel* **2005**, *84*, 53–61. [CrossRef]
9. Tor, H.O.; Arild, S.; Claas, V.D.Z.; Per, A.A. The Effect of Weighting Material Sag on Drilling Operation Efficiency. In Proceedings of the Asia Pacific Oil & Gas Conference & Exhibition, Jakarta, Indonesia, 30 October–1 November 2007.
10. Bern, P.A.; Van Oort, E.; Neustadt, B.; Ebeltoft, H.; Zurdo, C.; Zamora, M.; Slater, K.S. Barite Sag: Measurement, Modeling, and Management. *SPE Drill. Complet.* **2000**, *15*, 25–30. [CrossRef]
11. Jamrozik, A.; Gonet, A.; Fijał, J.; Terpiłowski, K.; Czekaj, L. Analysis of waste mud stability. *Wydaw. Agh* **2014**, *31*, 25. [CrossRef]
12. Santos, N.B.C.; Fagundes, F.M.; de Oliveira Arouca, F.; Damasceno, J.J.R. Sedimentation of solids in drilling fluids used in oil well drilling operations. *J. Pet. Sci. Eng.* **2018**, *162*, 137–142. [CrossRef]
13. Ofei, T.N.; Lund, B.; Saasen, A. Effect of particle number density on rheological properties and barite sag in oil-based drilling fluids. *J. Pet. Sci. Eng.* **2021**, *206*, 108908. [CrossRef]
14. Zeng, W.; Bouguetta, M. A Comparative Assessment of Barite SAG Evaluation Methods. In Proceedings of the SPE Deepwater Drilling and Completions Conference, Galveston, TX, USA, 14–15 September 2016.
15. Ribeiro, J.; Eler, F.; Martins, A.; Scheid, C.; Calçada, L.; Meleiro, L. A Simplified Model Applied to the Barite Sag and Fluid Flow in Drilling Muds: Simulation and Experimental Results. *Oil Gas Sci. Technol.* **2017**, *72*, 23. [CrossRef]
16. Wang, J.; Zhang, J.; Yan, L.; Cheng, R.; Ni, X.; Yang, H. Prevent Barite Static Sag of Oil-Based Completion Fluid in Ultra-Deep Wells. In Proceedings of the International Petroleum Technology Conference, Virtual, 23 March–1 April 2021.
17. Sentis, M.P.L.; Lemahieu, G.; Hemsley, E.; Bouzaid, M.; Brambilla, G. Size distribution of migrating particles and droplets under gravity in concentrated dispersions measured with static multiple light scattering. *J. Colloid Interface Sci.* **2024**, *653*, 11. [CrossRef]
18. Batchelor, G.K. (Ed.) Contents. In *An Introduction to Fluid Dynamics*; Cambridge University Press: Cambridge, UK, 2000; pp. v–xii.
19. Mills, P.; Snabre, P. Settling of a Suspension of Hard Spheres. *Europhys. Lett.* **2007**, *25*, 651. [CrossRef]
20. Bürger, R.; Fernández-Nieto, E.D.; Osores, V. A dynamic multilayer shallow water model for polydisperse sedimentation. *ESAIM Math. Model. Numer. Anal.* **2019**, *53*, 1391–1432. [CrossRef]
21. Mahyar, M.; Johnston, L.J.; Jakubek, Z.J. Dispersion, stability and size measurements for cellulose nanocrystals by static multiple light scattering. *Cellulose* **2018**, *25*, 5751–5768. [CrossRef]
22. Sentis, M.P.L.; Brambilla, G.; Fessard, V.; Meunier, G. Simultaneous screening of the stability and dosimetry of nanoparticles dispersions for in vitro toxicological studies with static multiple light scattering technique. *Toxicol. Vitr. Int. J. Publ. Assoc. BIBRA* **2020**, *69*, 104972. [CrossRef]
23. Storti, F. Particle size distributions by laser diffraction: Sensitivity of granular matter strength to analytical operating procedures. *Solid Earth* **2010**, *1*, 25–48. [CrossRef]
24. Haller, N.; Kulozik, U. Separation of Whey Protein Aggregates by Means of Continuous Centrifugation. *Food Bioprocess Technol.* **2019**, *12*, 1052–1067. [CrossRef]
25. Yang, Y.B.; Xiao, W.L.; Zheng, L.L.; Lei, Q.H.; Qin, C.Z.; He, Y.A.; Liu, S.S.; Li, M.; Li, Y.M.; Zhao, J.Z. Pore throat structure heterogeneity and its effect on gas-phase seepage capacity in tight sandstone reservoirs: A case study from the Triassic Yanchang Formation, Ordos Basin. *Pet. Sci.* **2023**, *20*, 2892–2907. [CrossRef]

26. Liu, P.; Yao, J.; Couples, G.D.; Huang, Z.; Sun, H.; Ma, J. Numerical modelling and analysis of reactive flow and wormhole formation in fractured carbonate rocks. *Chem. Eng. Sci.* **2017**, *172*, 143–157. [CrossRef]
27. Zhai, L.; Yang, M.; Yan, C.; Tian, T.; Huang, S. Dynamic Distribution Characteristics of Oil and Water during Water Flooding in a Fishbone Well with Different Branch Angles. *ACS Omega* **2022**, *7*, 27206–27215. [CrossRef]
28. Xiao, W.; Yang, Y.; Bernabé, Y.; Lei, Q.; Li, M.; Xie, Q.; Zheng, L.; Liu, S.; Huang, C.; Zhao, J. Experimental Study on EOR in Shale Oil Cores during Associated Gasflooding: A Case Study from Yanchang Formation, Ordos Basin. *SPE J.* **2023**, *28*, 17. [CrossRef]
29. Wang, Y.; Shang, Q.; Guo, J.; Zhou, L. Study on imbibition during the CO_2 enhanced oil recovery in fractured tight sandstone reservoirs. *Capillarity* **2023**, *7*, 47–56. [CrossRef]
30. Liu, P.; Yan, X.; Yao, J.; Sun, S. Modeling and analysis of the acidizing process in carbonate rocks using a two-phase thermal-hydrologic-chemical coupled model. *Chem. Eng. Sci.* **2019**, *207*, 215–234. [CrossRef]
31. Brandão Costa Santos, N.; Marques Fagundes, F.; Leibsohn Martins, A.; Ribeiro Damasceno, J.J.; de Oliveira Arouca, F. Stability of oil well olefin drilling fluids: Solid–liquid sedimentation and rheological characterization. *Part. Sci. Technol.* **2019**, *38*, 203–209. [CrossRef]
32. Deninno, E.; Molina, M.; Shipman, J.; Dearing, H.; Arpini, F.; Bussaglia, L. High Performance Water Base Fluid Improves Wellbore Stability and Lowers Torque. In Proceedings of the SPE/IADC Middle East Drilling Technology Conference & Exhibition, Abu Dhabi, United Arab Emirates, 26–28 January 2016.
33. Amin, M.; Fawzy, A.; Dawood, M.; Rahal, A.; Salazar, N.; Al Maktoum, F.; Al Kindi, M.; Al Rashdi, M. Nanotechnology-Driven Bridging Package Approach for Improving Wellbore Stability, Preventing Differential Sticking, and Reducing Loss Events in Severely Depleted Formations in Oman. In Proceedings of the SPE Conference at Oman Petroleum & Energy Show, Muscat, Oman, 12–14 May 2025.
34. Tu, J.; Fan, D.; Sun, F.; Kaminski, A.; Smyth, W. Shear Instabilities and Stratified Turbulence in an Estuarine Fluid Mud. *J. Phys. Oceanogr.* **2022**, *52*, 2257–2271. [CrossRef]
35. Meiburg, E.; Kneller, B. Turbidity Currents and Their Deposits. *Annu. Rev. Fluid Mech.* **2009**, *42*, 135–156. [CrossRef]
36. Angle, B.R.; Rau, M.J.; Byron, M.L. Settling of nonuniform cylinders at intermediate Reynolds numbers. *Phys. Rev. Fluids* **2024**, *9*, 070501. [CrossRef]
37. Nasr-Azadani, M.M.; Meiburg, E. Turbidity currents interacting with three-dimensional seafloor topography. *J. Fluid Mech.* **2014**, *745*, 409–443. [CrossRef]
38. Jiang, Y.; Wu, J.; Cheng, Q.; Yang, C.; Song, X. Gas Injection for Improving Oil Recovery in Highly Volatile Fractured Reservoirs with Thick Buried Hills in Bohai Sea. *J. Mar. Sci. Appl.* **2024**, 1–10. [CrossRef]
39. Feng, Y.; Mu, X.; Wang, B.; Tang, J.; Feng, T.; Xiang, J.; Peng, F. Study on the Geochemical Genesis and Differences of Ordovician Oil and Gas Reservoirs. *Chem. Technol. Fuels Oils* **2024**, *59*, 1175–1183. [CrossRef]

Disclaimer/Publisher's Note: The statements, opinions and data contained in all publications are solely those of the individual author(s) and contributor(s) and not of MDPI and/or the editor(s). MDPI and/or the editor(s) disclaim responsibility for any injury to people or property resulting from any ideas, methods, instructions or products referred to in the content.